Heterogeneous Inertial Measurement Units in Motion Analysis

Filip Malawski[a] and Natalia Paruzel-Satława

Institute of Computer Science, AGH University of Science and Technology, Krakow, Poland

Abstract: Inertial measurement units are commonly used in motion analysis applications, such as sports training aid, gait analysis, medical diagnosis, or rehabilitation assistance. Linear acceleration and orientation obtained from sensor fusion are employed for the detection and classification of actions, as well as for measuring relevant parameters of the motion. Typically, in multi-sensor setups, a single model of the device is used. However, considering potential end-users, it could be beneficial to allow heterogeneous setups, particularly by including everyday-use devices with built-in inertial sensors, such as smartwatches. In this work, we perform experiments with several different sensors in order to analyze agreement in their measurements. Results indicate that devices of different models are not directly interchangeable, however, in some applications, heterogeneous setups may be viable.

1 INTRODUCTION

Inertial measurement units (IMU) measure acceleration and angular velocity, as well as, in the case of most such devices, magnetic field. Moreover, a fusion of those data modalities provides an estimation of 3D orientation, relevant for many motion analysis applications. A number of methods for motion analysis have been proposed in the literature (Lopez-Nava and Munoz-Melendez, 2016), however it is a common practice, that the data for the experiments are collected with homogeneous devices. From a practical point of view, a question arises - once we substitute an IMU with a different model will the proposed methods work the same? Moreover, what if we were to use a heterogeneous setup, with multiple IMU models working in parallel? Recently, more and more everyday-use devices have built-in IMUs (e.g. smartphones, smartwatches, fitness bands). Employing those as part of a multi-sensor motion analysis system would be beneficial for the end user, as it would reduce the number and therefore the cost of additional devices needed to purchase in order to use such a system. In this work, we perform a series of experiments to verify the potential interchangeability of different IMU sensors in motion analysis applications, including two dedicated IMU models and one smartwatch.

2 RELATED WORKS

IMUs are commonly used for motion analysis in applications such as sports action recognition and evaluation, gait analysis, as well as rehabilitation exercise assistance. In sports, IMUs are used in a wide range of disciplines, both practiced indoors, such as combat sports (Worsey et al., 2019a), volleyball (Wang et al., 2018) or basketball (Ren and Wang, 2021), and outdoors, such as rowing (Worsey et al., 2019b) or football (Wilmes et al., 2020). Aside from event detection and classification, depending on the discipline, a number of useful motion parameters are extracted, including velocity, acceleration, cycle length, amplitude, angular displacement, force, and others (Camomilla et al., 2018).

Gait analysis is often a useful tool in medical diagnosis, including degenerative joint diseases such as osteoarthritis (Kobsar et al., 2020), as well as neurological impairments, such as Parkinson's disease (Tunca et al., 2017; Petraglia et al., 2019). Measured parameters include, among others, stride and step length, cadence, speed, as well as cycle, stance, and swing times (Teufl et al., 2018).

In rehabilitation, motion analysis with IMUs is employed, among others, for the classification of shoulder activities in guided treatment (Bavan et al., 2019), detection of correct and incorrect performance of lower limb exercises (Giggins et al., 2014), as well as tracking specific exercises to aid stroke pa-

[a] https://orcid.org/0000-0003-0796-1253

tients (Zhou et al., 2006). Angles of joint movement are most often of interest in rehabilitation scenarios (Milosevic et al., 2020).

While some works show successful applications of a single IMU sensor, e.g. for knee rehabilitation monitoring (Bevilacqua et al., 2018) or swimming motion analysis (Wang et al., 2019), most solutions require a multi-sensor setup. Review papers indicate, that there are at least several popular IMU devices, dedicated to motion analysis, available on the market (Petraglia et al., 2019; Milosevic et al., 2020). However, closer inspection reveals, that most of them are high-cost, advanced devices targeted for research or professional medical and sports applications. In this work, we focus on relatively low-cost devices, that are affordable for a home-use scenario. It is worth noting, that in the referenced works, all multi-sensor solutions employ homogeneous setups, with a single model of IMU. While there are studies focused on the validation of IMUs against optical systems (Roell et al., 2019; Malawski, 2020; Clemente et al., 2022), there's a lack of works employing multiple different IMUs together. In this study, we consider a heterogeneous setup, in which multiple different devices could cooperate, including everyday-use equipment such as smartwatches. To the best of our knowledge, there are no previous works performing similar analyses.

3 METHODS

3.1 Sensors

Our goal is to compare low-cost devices, that could be used in consumer-level applications. We employ Xsens DOT[1] and MBientLab MeatMotionRL[2] sensors, both priced approx. 100 USD per device. Moreover, we also include in our experiments Samsung Galaxy Watch 4 smartwatch[3], in order to verify if everyday-use devices equipped with IMUs could be employed in motion analysis setups as well. Employed sensors are depicted in Fig. 1.

Xsens DOT is a small (36x30x11mm) and light (11g) device, providing measurements of orientation, acceleration (±16g), angular velocity ($\pm2000°$/s), and magnetic field ($\pm$ 8 Gauss), either in real-time streaming (up to 60Hz) or by recording to internal memory (up to 120Hz). It is equipped with a BLE 5.0 communications module. MetaMotionRL sensor is a similar device, with comparable size (36x27x10mm)

and weight (8.5g), providing the same set of information, however in a more configurable manner. Available accelerometer ranges span from ±2g to ±16g, gyroscope ranges span from $\pm125°$/s to $\pm2000°$/s and magnetometer is fixed at ±13 Gauss for x and y axes and ±25 Gauss for z axis. Acceleration, angular velocity, and orientation can be streamed in real-time at 100Hz, or logged with 800Hz. MetaMotionRL is equipped with older BLE 4.0. Both sensors have APIs available for multiple programming languages, supporting both desktop and mobile development of applications. As for the Samsung Galaxy Watch 4 (40x40x10mm, 26g), very little information is provided regarding the built-in IMU. Acceleration, angular velocity, magnetic field, and orientation are all available through Android API, as the smartwatch runs on Wear OS - a version of Android dedicated to wearable devices. The sampling frequency is not given explicitly, although experiments indicate that it is possible to obtain data with as much as 100Hz frequency using Android's *SENSOR_DELAY_FASTEST* setting. However, due to large fluctuations of sampling times, it seems more reasonable to use *SENSOR_DELAY_GAME* setting, which effectively results in a 50Hz sampling rate.

Figure 1: Sensors used in the experiments, left to right: MBientLab MetaMotionRL, Xsens DOT, Samsung Galaxy Watch 4.

3.2 Acquisition

In our experiments, we employ a total of four sensors: two Xsens DOT devices, one MetaMotionRL, and one Galaxy Watch 4. This allows us to measure and compare the similarity of signals acquired with sensors of the same model, and of different models. In order to obtain comparable measurements of the same motion, the sensors are mounted on top of each other, along the shorter z-axis, with separation layers made of technical foam, and strong non-elastic tape used to hold them together. Therefore, all sensors are moved as a single bundle. All devices are calibrated as indicated by their producers. For the Xsens DOT, we use acquisition software provided with the sensors, for the MetaMotionRL we use custom software employing programming libraries provided with the sensor, and for the Galaxy Watch 4 we use custom

---

[1]https://www.xsens.com/xsens-dot

[2]https://mbientlab.com/store/metamotionrl-p/

[3]https://www.samsung.com/us/watches/galaxy-watch4/

Android-based software.

We consider two experimental scenarios. In the first one, we focus on acceleration in linear motion. The sensor bundle is moved, separately, in three directions (left-right, up-down, forward-backward), without rotations. The sequence is repeated three times with different speeds, to collect data points in various parts of the available measurement range. We record so-called linear acceleration, which is acceleration with removed gravity - all employed devices have a built-in capability of such filtering.

The second scenario is focused on orientation. The sensor bundle is rotated, in two directions, in half-circle arcs with a radius of approx. 50cm. The motion is repeated at 3 different speeds. We record Euler angles, provided by each sensor's built-in fusion algorithm, as those are easier to interpret than quaternions. Fusion makes use of all raw signals - acceleration, angular velocity, and magnetic field.

3.3 Synchronization

Synchronization of data is one of the key requirements in a multi-sensor setup. This is typically done by synchronizing internal clocks and then providing a timestamp for each measured data point (Khediri et al., 2012). Both Xsens DOT and MetaMotionRL sensors have built-in synchronization protocols, which could be employed in a homogeneous setup. For heterogeneous setup, implementing clock synchronization on multi-vendor devices would require low-level programming of acquisition software for each device. Instead, for our experiments, we employ signal-based synchronization, which handles clock drift between sensors using the acquired data, rather than communication between devices. Each recording is started with the sensor bundle in a stationary position, then a short-term force is applied (a single push), then for a few seconds the sensors are left stationary again, then the actual movement for the experiments starts. At the end of each recording similar protocol is followed (a single push with no movement before and after). A single push is easily identified as a single peak in the acceleration signal (see Fig. 2 - first and last peak of each signal). Therefore, we can synchronize the data from all sensors, by selecting only fragments between the first and the last peak, with a given threshold for the peak height.

This procedure ensures, that in the trimmed data, the start and end time points are the same for each sensor. However, we still need to address different sampling rates and spacing of the timestamps. DOT and MetaMotionRL provide data points evenly distributed in time, however, Android API does not. Therefore,

data points for Galaxy Watch 4 were determined in evenly distributed time points by taking the weighted average of the nearest measured data points. In order to obtain a common sampling rate, we resample the MetaMotionRL and Galaxy Watch 4 data to 60Hz, which is native to the DOT sensors. Finally, we remove leading and trailing close-to-zero signal fragments, which result from maintaining a stationary position near the synchronization peaks (see Fig. 3).
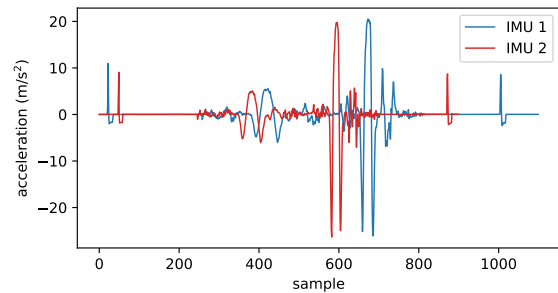

Figure 2: Acceleration (single axis) acquired at the same time with two different IMUs - before synchronization.
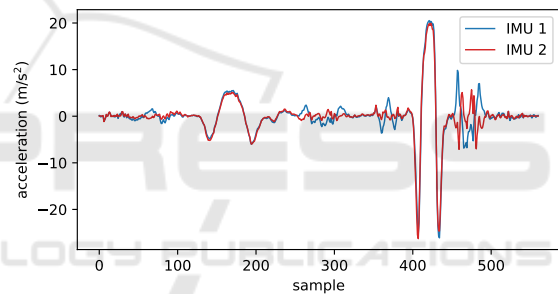

Figure 3: Acceleration (single axis) acquired at the same time with two different IMUs - after synchronization.

3.4 Processing

For better comparison of the sensors, we apply processing to the raw acquired data. The acceleration signal is very noisy, therefore it is a common approach to apply filtering methods to the raw data. We decided to use basic running average filtering with window size 7, in order to make the signals easier to compare on the plots representing values in time. Running average results in low-pass filtering, which in this case is desirable, as high frequencies correspond mostly to noise, and lower frequencies correspond to actual actions performed in the experiments.

In the case of orientation, Euler angles are provided in the range (-180°, 180°). Once the device is rotated outside of this range (less than -180° or more than 180°) the fusion algorithm returns an equivalent value inside the range, e.g. -175° instead of 185° (see the raw signal in Fig. 4). This makes it difficult to

analyze such data, as large numeric differences between values in two signals may actually represent a very small difference in measurement, e.g. 179° vs. -179° is in fact just 2° of difference, not 358°. For this reason, we apply dedicated processing in the orientation experiments. In each signal, we search for data points in which the transition between the end of the positive and the start of the negative range occurs. These are easy to find as high peaks in the difference of consecutive values. In segments located between such data points, we add the full range (360°) to the recorded values. Therefore, we obtain continuous signals (see. processed data in Fig. 4). We additionally apply running average filtering, with windows size 7, to remove unwanted peaks that may still occur near the transition points.
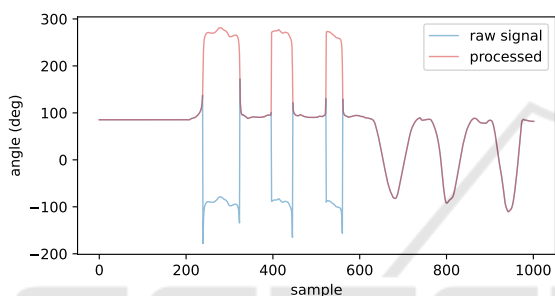

Figure 4: Raw and processed orientation data (single axis).

3.5 Metrics

As the first indication of similarity between signals from different devices, we analyze plots representing measured values in time. We compare against the first Xsens sensor, denoted as DOT (1), all other sensors: the second Xsens device, denoted as DOT (2), the MetaMotionRL sensor, and the Galaxy Watch 4. Then, we measure the numeric difference of measurements in corresponding time points. For the orientation data, we consider point-by-point differences (60Hz sampling). Acceleration data, however, even after employing running average filtering, remains too noisy to be directly compared. Instead, for numerical analysis, we compute the mean value of the raw signal in time windows of size 16, and overlap of half window length. This corresponds to the common technique of extracting time-domain features from the acceleration data (O'Reilly et al., 2018). We then measure the difference between values computed in the corresponding windows.

The mean and the standard deviation of difference are computed and presented as numerical results. We also include Bland-Altman plots, in which the difference between two paired measurements is plotted

against their mean. Bland-Altman plots are commonly used to depict agreement between different measurement methods. For normally distributed data agreement limits (dashed horizontal lines) are typically set to 1.96 of standard deviation, to include 95% of data points. In our experiments, the differences are not normally distributed (based on the Shapiro-Wilk test), therefore we compute agreement limits specifically to contain 95% of data points (per each signal-to-signal comparison).

4 EXPERIMENTS

Performed experiments included the two scenarios described in Section 3.2, focusing on measurements of 1) acceleration in linear motion and 2) orientation. Agreement between multiple repetitions of motion in the same scenario was not considered in this work. The duration of acquired signals was approx. 15 seconds.

4.1 Linear Acceleration

For brevity, we present filtered signal comparison in the x-axis only, including DOT (1) vs. DOT (2) (Fig. 5), DOT (1) vs. MetaMotionRL (Fig. 6) and DOT (1) vs. Galaxy Watch 4 (Fig. 7). Raw signals are additionally depicted with half-opacity dotted lines to indicate the impact of the running average filtering. The Bland-Altman plot (Fig. 8) includes data points from all axes. Each comparison (sensor pair) is indicated with a different color.
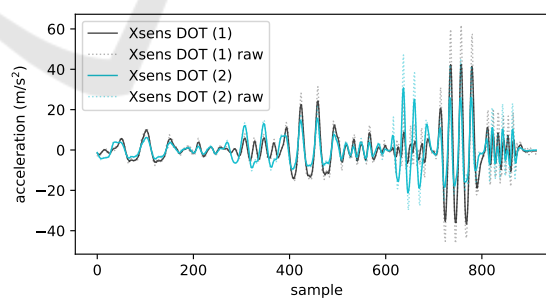

Figure 5: Linear acceleration, x-axis, Xsens DOT (1) vs. Xsens DOT (2).

Visual inspection of linear acceleration values in time indicates that signals are generally well-aligned in terms of peaks occurring at the same time points. However, the magnitude of peaks varies, particularly in data fragments with fast motion. This can be observed in all comparisons - between the same device model (Fig. 5), as well as with different models (Fig. 6 and 7). Numerical results (Tab. 1), as well as
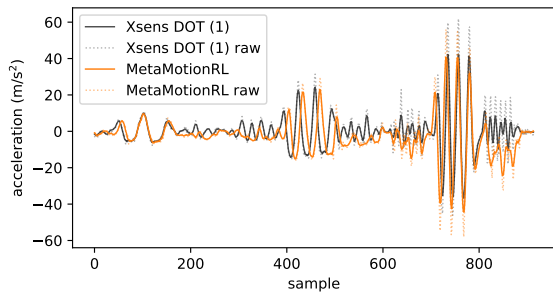
Figure 6: Linear acceleration, x-axis, Xsens DOT (1) vs. MetaMotionRL.
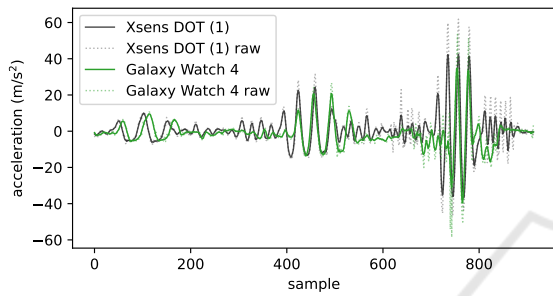

Figure 7: Linear acceleration, x-axis, Xsens DOT (1) vs. Galaxy Watch 4.
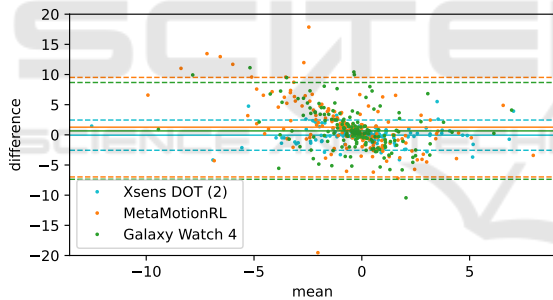

Figure 8: Bland-Altman plot representing agreement in measurements of linear acceleration (in time windows), all axes, Xsens DOT (1) vs. all other sensors.

the Bland-Altman plot (Fig. 8), indicate that there is much better agreement between measurements performed with devices of the same model. Considering the two other devices, the mean difference from values measured with the baseline sensor is better in the case of Galaxy Watch 4 ($0.65 m/s^2$) than in the case of MetaMotionRL ($1.27 m/s^2$). On the other hand, the standard deviation is very similar ($4.21 m/s^2$ and $4.09 m/s^2$ respectively) and so are the agreement limits including 95% of data points (see Fig.8).

4.2 Orientation

Similarly, as in the case of linear acceleration, we present signal comparison only in the x-axis to keep

Table 1: Mean and standard deviation values of difference in measuring linear acceleration (m/s^2) between Xsens DOT (1) and all other sensors, computed in time windows.

Sensor	Mean	Std
Xsens DOT (2)	-0.05	1.28
MetaMotionRL	1.27	4.21
Galaxy Watch 4	0.65	4.09

this section concise. We include orientation data for DOT (1) vs. DOT (2) (Fig. 9), DOT (1) vs. MetaMotionRL (Fig. 10), and DOT (1) vs. Galaxy Watch 4 (Fig. 11). Raw signals are depicted with half-opacity dotted lines. Numerical results (Tab. 2) and the Bland-Altman plot (Fig. 12) include data from the x-axis only. An additional close-up view of a smaller range is depicted in Fig. 13.
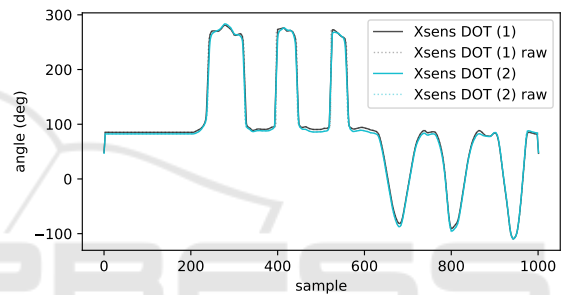

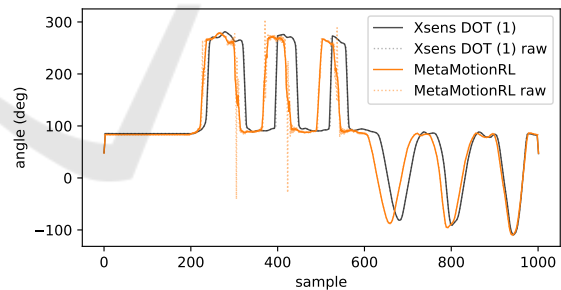Figure 9: Orientation, x-axis, Xsens DOT (1) vs. Xsens DOT (2).

Figure 10: Orientation, x-axis, Xsens DOT (1) vs. MetaMotionRL.

In the plots depicting orientation value in time we can observe, that alignment with the baseline DOT (1) sensor data is near perfect for both DOT (2) and Galaxy Watch 4 devices (Fig. 9 and 11). However, it is worth noting, that the Galaxy Watch 4 requires running average filtering, as the raw data have some undesirable peaks, while DOT (2) provides a smooth signal by itself. MetaMotionRL sensor produces similar peaks as the other devices, although some of them are shifted in time (Fig. 10). This is most likely due to different sensor fusion algorithms - there is always
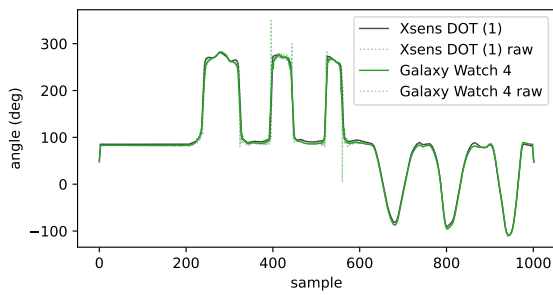
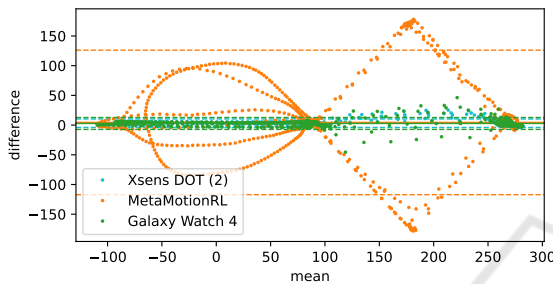Figure 11: Orientation, x-axis, Xsens DOT (1) vs. Galaxy Watch 4.

Figure 12: Bland-Altman plot of orientation, x-axis, Xsens DOT (1) vs. other sensors, full range.
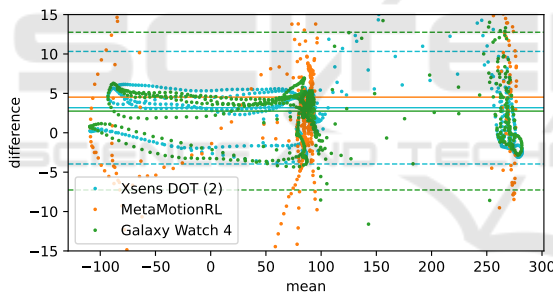

Figure 13: Bland-Altman plot of orientation, x-axis, Xsens DOT (1) vs. other sensors, selected range.

a trade-off between accuracy and delay in computing orientation from the noisy, raw, multi-modal signals. Please note, that in this work we do not evaluate which device has better consistency with a gold standard measurement, but rather measure agreement between the sensors, therefore we do not conclude which data is more correct.

Results in Tab. 2, as well as the close-up of the Bland-Altman plot (Fig. 13) also indicate very good agreement between DOT (1) and both DOT (2) and Galaxy Watch 4 sensors. The latter has a lower mean difference (2.75° vs. 3.18°), but a higher standard deviation (5.11° vs. 3.64°). MetaMotionRL has a very high standard deviation of difference (62.10°), as a result of the observed time shift. However, the mean difference (4.52°) is comparable with the other sen-

Table 2: Mean and standard deviation values of difference in measuring orientation (degrees) between Xsens DOT (1) and all other sensors.

Sensor	Mean	Std
Xsens DOT (2)	3.18	3.64
MetaMotionRL	4.52	62.10
Galaxy Watch 4	2.75	5.11

sors, due to the circular nature of the motion. The time shift is also well visible on the full-range Bland-Altman plot (Fig. 12).

4.3 Discussion

Based on the obtained results, we can conclude that in the case of linear acceleration, we cannot easily substitute one model of IMU with another, as measurements will differ. Depending on the application, these differences may be less or more significant. In particular, when relatively slow motion is considered, measurements seem to be more consistent. In applications including very dynamic motion, such as some sports disciplines, a per-sensor adaptation of data processing methods may be required, to compensate for the difference in measurements. On the other hand, for scenarios with less dynamic motion, such as daily activity recognition, those differences may be insignificant. While recording actual actions was out of the scope of this work, it would be interesting to compare differences between sensors to differences between subjects in the context of the type of performed motion. It is also worth noting that both a dedicated IMU (MetaMotionRL) and a smartwatch (Galaxy Watch 4) have a very similar agreement with the baseline DOT sensor.

Interestingly, considering orientation, measurements from the smartwatch are much more consistent with the baseline, than the MetaMotionRL IMU. We expect that, in terms of orientation, Galaxy Watch 4 could be directly used with motion analysis algorithms developed using the DOT sensors. On the other hand, the time shift occurring between the DOT and MetaMotionRL data may be difficult to compensate for. Using a custom fusion algorithm instead of the provided one could be considered. Some applications may not require very dynamic measurements of orientation, e.g. rehabilitation exercises are usually performed relatively slowly, therefore precise synchronization in time may be less relevant than the range of motion.

5 CONCLUSIONS

In this work, we performed experiments to analyze the agreement between measurements obtained with the same and different models of IMUs. We included dedicated inertial sensors as well as a common model of a smartwatch. Results indicate, that while the agreement is relatively good, it is not sufficient to simply substitute a device with another model or use a heterogeneous setup without additional consideration. However, in some applications, with proper adaptation, using multiple different sensors could be a viable solution. More importantly, from a practical point of view, employing an everyday-use device such as a smartwatch is just as good (or even better) as using another model of IMU. Discrepancies between measurements obtained with different devices are more significant in dynamic motion. Therefore, in scenarios such as analyzing fast, sports actions it may be necessary to calibrate motion analysis methods per device.

In terms of future work, it would be beneficial to verify the repeatability of measurements per device, as well as perform experiments with additional devices. We also consider comparing signals from different sensors as inputs to machine learning methods for action detection or classification. Such experiments would include multiple subjects. Training machine learning models on one set of sensors and testing on another would be a good indication of the viability of heterogeneous setups in practical scenarios.

ACKNOWLEDGEMENTS

REFERENCES

Bavan, L., Surmacz, K., Beard, D., Mellon, S., and Rees, J. (2019). Adherence monitoring of rehabilitation exercise with inertial sensors: A clinical validation study. *Gait & posture*, 70:211–217.

Bevilacqua, A., Huang, B., Argent, R., Caulfield, B., and Kechadi, T. (2018). Automatic classification of knee rehabilitation exercises using a single inertial sensor: A case study. In *2018 IEEE 15th International Conference on Wearable and Implantable Body Sensor Networks (BSN)*, pages 21–24. IEEE.

Camomilla, V., Bergamini, E., Fantozzi, S., and Vannozzi, G. (2018). Trends supporting the in-field use of wearable inertial sensors for sport performance evaluation: A systematic review. *Sensors*, 18(3):873.

Clemente, F., Badicu, G., Hassan, U., Akyildiz, Z., Pino-Ortega, J., Silva, R., and Rico-González, M. (2022). Validity and reliability of inertial measurement units for jump height estimations: a systematic review. *Human Movement*, 23(4):1–20.

Giggins, O. M., Sweeney, K. T., and Caulfield, B. (2014). Rehabilitation exercise assessment using inertial sensors: a cross-sectional analytical study. *Journal of neuroengineering and rehabilitation*, 11(1):1–10.

Khediri, S. e., Nasri, N., Samet, M., Wei, A., and Kachouri, A. (2012). Analysis study of time synchronization protocols in wireless sensor networks. *arXiv preprint arXiv:1206.1419*.

Kobsar, D., Masood, Z., Khan, H., Khalil, N., Kiwan, M. Y., Ridd, S., and Tobis, M. (2020). Wearable inertial sensors for gait analysis in adults with osteoarthritis—a scoping review. *Sensors*, 20(24):7143.

Lopez-Nava, I. H. and Munoz-Melendez, A. (2016). Wearable inertial sensors for human motion analysis: A review. *IEEE Sensors Journal*, 16(22):7821–7834.

Malawski, F. (2020). Depth versus inertial sensors in real-time sports analysis: a case study on fencing. *IEEE Sensors Journal*, 21(4):5133–5142.

Milosevic, B., Leardini, A., and Farella, E. (2020). Kinect and wearable inertial sensors for motor rehabilitation programs at home: state of the art and an experimental comparison. *Biomedical engineering online*, 19(1):1–26.

O'Reilly, M., Caulfield, B., Ward, T., Johnston, W., and Doherty, C. (2018). Wearable inertial sensor systems for lower limb exercise detection and evaluation: a systematic review. *Sports Medicine*, 48(5):1221–1246.

Petraglia, F., Scarcella, L., Pedrazzi, G., Brancato, L., Puers, R., and Costantino, C. (2019). Inertial sensors versus standard systems in gait analysis: a systematic review and meta-analysis. *European journal of physical and rehabilitation medicine*, 55(2):265–280.

Ren, H. and Wang, X. (2021). Application of wearable inertial sensor in optimization of basketball player's human motion tracking method. *Journal of Ambient Intelligence and Humanized Computing*, pages 1–15.

Roell, M., Mahler, H., Lienhard, J., Gehring, D., Gollhofer, A., and Roecker, K. (2019). Validation of wearable sensors during team sport-specific movements in indoor environments. *Sensors*, 19(16):3458.

Teufl, W., Lorenz, M., Miezal, M., Taetz, B., Fröhlich, M., and Bleser, G. (2018). Towards inertial sensor based mobile gait analysis: Event-detection and spatio-temporal parameters. *Sensors*, 19(1):38.

Tunca, C., Pehlivan, N., Ak, N., Arnrich, B., Salur, G., and Ersoy, C. (2017). Inertial sensor-based robust gait analysis in non-hospital settings for neurological disorders. *Sensors*, 17(4):825.

Wang, Y., Zhao, Y., Chan, R. H., and Li, W. J. (2018). Volleyball skill assessment using a single wearable mi-

cro inertial measurement unit at wrist. *IEEE Access*, 6:13758–13765.

Wang, Z., Shi, X., Wang, J., Gao, F., Li, J., Guo, M., Zhao, H., and Qiu, S. (2019). Swimming motion analysis and posture recognition based on wearable inertial sensors. In *2019 IEEE International Conference on Systems, Man and Cybernetics (SMC)*, pages 3371–3376. IEEE.

Wilmes, E., de Ruiter, C. J., Bastiaansen, B. J., Zon, J. F. v., Vegter, R. J., Brink, M. S., Goedhart, E. A., Lemmink, K. A., and Savelsbergh, G. J. (2020). Inertial sensor-based motion tracking in football with movement intensity quantification. *Sensors*, 20(9):2527.

Worsey, M. T., Espinosa, H. G., Shepherd, J. B., and Thiel, D. V. (2019a). Inertial sensors for performance analysis in combat sports: A systematic review. *Sports*, 7(1):28.

Worsey, M. T., Espinosa, H. G., Shepherd, J. B., and Thiel, D. V. (2019b). A systematic review of performance analysis in rowing using inertial sensors. *Electronics*, 8(11):1304.

Zhou, H., Hu, H., and Harris, N. (2006). Application of wearable inertial sensors in stroke rehabilitation. In *2005 IEEE Engineering in Medicine and Biology 27th Annual Conference*, pages 6825–6828. IEEE.